analytical chemistry

Article

pubs.acs.org/ac

Highly Ordered Silicon Pillar Arrays As Platforms for Planar Chromatography

Teresa B. Kirchner,[†] Nahla A. Hatab,[†] Nickolay V. Lavrik,[‡] and Michael J. Sepaniak*[,†]

[†]Department of Chemistry, University of Tennessee, Knoxville, Tennessee 37996, United States

[‡]Center for Nanophase Materials Sciences, Oak Ridge National Laboratory, Oak Ridge, Tennessee 37830, United States

ABSTRACT: Unlike HPLC, there has been sparse advancement in the stationary phases used for planar chromatography. Nevertheless, modernization of planar chromatography platforms can further highlight the technique's ability to separate multiple samples simultaneously, utilize orthogonal separation formats, image (detect) separations without rigorous temporal demands, and its overall simplicity. This paper describes the fabrication and evaluation of ordered pillar arrays that are chemically modified for planar chromatography and inspected by fluorescence microscopy to detect solvent development and analyte bands (spots). Photolithography, in combination with anisotropic deep reactive ion etching, is used to produce uniform high aspect ratio silicon pillars. The pillar heights, diameters, and pitch variations are approximately 15−20 μm, 1−3 μm, and 2−6 μm, respectively, with the total pillar array size typically 1 cm × 3 cm. The arrays are imaged using scanning electron microscopy in order to measure the pillar diameter and pitch as well as analyze the pillar sidewalls after etching and stationary phase functionalization. These fluidic arrays will enable exploration of the impact on mass transport and chromatographic efficiency caused by altering the pillar array morphology. A C18 reverse stationary phase (RP), common RP solvents that are transported by traditional but uniquely rapid capillary flow, and Rhodamine 6G (R6G) as the preliminary analyte are used for this initial evaluation. The research presented in this article is aimed at understanding and overcoming the unique challenges in developing and utilizing ordered pillar arrays as a new platform for planar chromatography: focusing on fabrication of expansive arrays, studies of solvent transport, methods to create compatible sample spots, and an initial evaluation of band dispersion.

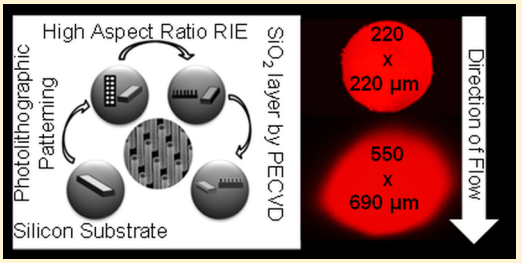

Modification of fabrication processes traditionally designed for the semiconductor industry has been shown to have advantages in the development of on-chip separation techniques. Using these techniques allows for the fabrication of micro- and nano-structured on-chip separation media that have been proven to be successful using computational analysis and actual separations by Desmet et al.[1−4] This approach was pioneered by Regnier and co-workers in the late 1990s,[5,6] who fabricated pillar arrays within channels in a reproducible and controlled manner. The advantages of using ordered arrays comprised of high aspect ratio pillars as a separation medium over traditional packed and monolithic columns have been well documented.[1,6−8] Significantly, separation efficiency with these engineered systems is usually improved when replacing relatively polydisperse and heterogeneous packing particles with lithographically fabricated pillars. The separation media in packed and monolithic columns realize benefits in mass transfer related efficiency as the size of the media particles or domains becomes smaller. However, scaling down traditional systems generally exasperates nonuniformity of the packing itself and the beds created with them and also increases pressure demands. Conversely, an advantage identified in recent studies is that nearly perfect ordered pillar arrays exhibit less flow resistance than comparable traditional packed and monolithic columns.[9] The improved flow resistance of these pillar array systems coupled with the ability to greatly reduce the pillar size to low-micro- or nanoscale indicates that this separation platform should exhibit an improvement over traditional separation media. Moreover, in a practical sense, these diminutive lab-on-a-chip platforms are expected to be particularly useful for in-field monitoring or point-of-care diagnostics due to the overall simplicity of the device. The footprint of the device is small, allowing for ease of transport, the system is reusable which offsets production costs, and only small sample volumes are required for analysis.

Appropriately designed pillar arrays have enabled novel separation mechanisms. An example is the use of deterministic lateral displacement discovered for particle separation accomplished by manipulating pillar positions to cause separations by altering the path taken by varying particles.[10] More conventional separation methods have also been used that are more similar to packed bed liquid chromatography which combines a mobile phase-stationary phase partitioning type separation which is controlled by the retentive nature of the solute within the system. Examples of these include pressure driven separations in pillar array systems explored by Desmet and coworkers using C8 and C18 liquid phase modifications with both porous and nonporous pillar arrays.[3,7,11,12] These examples highlight the possibility of using pillar array separation

Received: July 22, 2013
Accepted: November 14, 2013

   dx.doi.org/10.1021/ac402261p | *Anal. Chem.* XXXX, XXX, XXX−XXX

platforms on real world samples while recognizing the challenges that impede these substrates from being competitive with traditional packed bed columns. These challenges include increasing the pillar surface area in order to obtain a similar mass loadability as conventional HPLC columns, mechanical stability, and stationary phase creation. Theory predicts that by increasing the pillar surface area of these ordered arrays, results similar to HPLC can be achieved.[1,4] Electrochemical anodization has been proven to be a successful treatment to increase the surface area of pillar arrays,[2,13] and more recently sol−gel chemistry has been effectively used on silicon pillar arrays for separations.[14] Stationary phase functionalization in pillar array systems using standard reverse phases can be complicated in that occlusion can occur in the system obstructing solvent flow so advances in this area are critical.

Our research group has addressed methods to increase mechanical stability and phase functionalization using pillar arrays for separations in pressurized systems.[15,16] These include capping the pillar array with silicon oxide in order to increase the robustness of the array and using a gas phase stationary phase modification to functionalize the pillar array surface creating a reverse phase. However, because of the challenges of sealing these pressurized devices, we have expanded our research herein to include nonpressurized planar chromatography.

Recent advances in ultrathin layer chromatography (UTLC) indicate that ultrathin layers improve efficiency of planar chromatography while decreasing development time and solvent volume. Notable examples are electrospun polymer layers[17] and electron-beam evaporation of thin SiO_2 layers.[18] Other research indicates that advances in the substrates used for capillary flow chromatography show promising results in advancing the technology used in planar chromatography.[9] Additional modern advances have occurred in TLC including reduction in particle size (high performance versions, i.e., HPTLC), overpressure and electrokinetically driven development, and the aforementioned UTLC.[9,19−20] Herein we present for the first time original research using lithographically fabricated uniform pillar arrays for planar chromatography in an open format that are driven by simple capillary action flow. It should be noted that benefits of moderate heterogeneity have been recently reported by Tallarek and co-workers where simulations indicate that at high velocities transverse transport in regular pillar arrays is lacking.[21] These confined pillar array systems as well as spherical particles in tubes, benefit from a small amount of disorder within the system to promote transverse transport and mitigate confinement related dispersion. However, for our unconfined, unpressurized systems with relatively low flow velocities it is not clear that the advantages of moderate disorder are relevant.

Moreover, with open format systems we expect to alleviate some of the problematic issues with pressurized pillar arrays in channels and create new opportunities such as orthogonal 2-D separations and simplified detection. However, the reduction in size and volume of our lithographic-based pillar array platforms relative to traditional TLC creates its own experimental challenges such as uniformly fabricating pillar arrays of >1 cm^2, dealing with heightened solvent evaporation, and the need for introducing very small sample spots. The focus of the current work is fabrication of expansive pillar arrays, studies of solvent transport, methods to create compatible sample spots, and an initial evaluation of band (spot) dispersion.

EXPERIMENTAL SECTION

Chip Design and Fabrication of Open Pillar Arrays for Separations. To fabricate the initial generation of these planar pillar arrays, a modified version of the technique described in previous publications to generate high-aspect ratio pillar arrays for pressurized systems was used.[16] Standard cleanroom lithographic processing techniques were used in the fabrication process as depicted in Figure 1. Czochralski

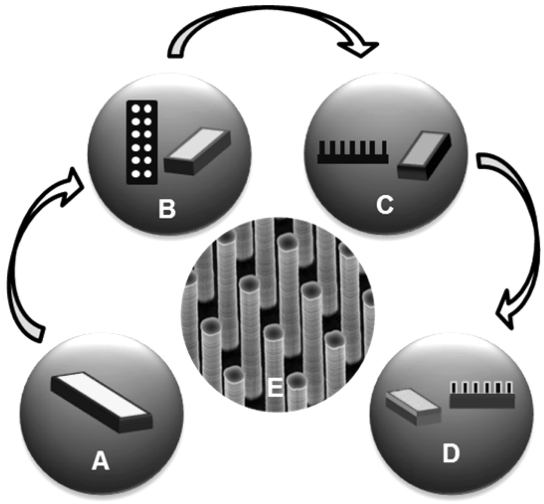

Figure 1. Fabrication sequence starts with a silicon wafer substrate (A) on which photolithographic patterning is performed (B) followed by DRIE (C) to create the high aspect ratio pillars which are coated with silicon oxide via PECVD (D). An SEM of typical array is shown in part E.

grown (p-type) 100 mm silicon wafers were used for our top down fabrication process, having an (100) orientation, a thickness ranging from 300 to 500 μm and resistivity between 0.01 and 20 Ω cm.

The 100 mm diameter allowed for 10 chips per wafer that were a 3 cm × 1 cm in area. The entire 3 cm^2 chip is a highly ordered array of pillars (Figure 2). The pillars were arrayed using CAD software defining the pillars as rhomboids laid out

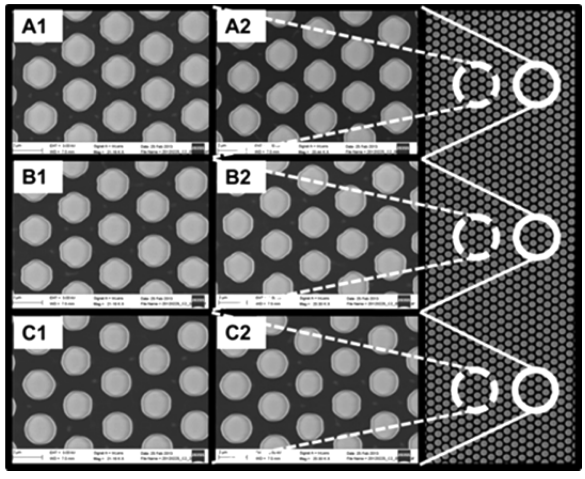

Figure 2. SEM images of a typical pillar array (pillar dimension of 2 μm with 2 μm pitch). Images A−C are the enlarged areas of the array (right) to show pillar uniformity.

dx.doi.org/10.1021/ac402261p | Anal. Chem. XXXX, XXX, XXX−XXX

in equilateral triangles, as discussed by Desmet and co-workers[1] using eq 1,

$$P = [(2G + 2D)^2 - (G + D)^2]^{1/2} \quad (1)$$

where G is the gap between the pillar sidewalls, D is the pillar diameter, and P is the pitch of the pillars. The pillar array parameters that were investigated are listed in Table 1.

Table 1. Parameters for Arrays Investigated

chip description (all values micrometers)		$V_P N_P$[a]	(V_P/V_C)[b] × 100	$SA_T = SA_P N_P$[c]
pillar	gap	total pillar volume (TV_P)	void volume (%)	surface area/chip (× 10^9)
1	1	1.09 × 10^9	77	4.4
2	1	1.93 × 10^9	60	3.9
2	2	1.09 × 10^9	77	2.2
2	3	6.96 × 10^8	86	1.4
3	3	1.09 × 10^9	77	1.5

[a] V_P indicates the individual pillar volume and N_P is the total number of pillars per array. [b] V_C is the total volume per pillar array. [c] SA_T is the total surface area calculated by multiplying the surface area per pillar (SA_P) by the total number of pillars per array.

To analyze the reduced particle size effect we have varied the pillar dimensions and spacing. The pillar arrays were designed with pillar sizes that range from 1 to 3 μm with a pitch of 2−6 μm. To compare these systems with regular packed columns we calculated the external porosity by subtracting the volume of the pillars from the total volume of the chip and determined that this value was comparable to that for some packed columns. The surface area for each pillar array was also approximated in order to estimate analyte loadability and in order to determine concentration volumes for the surface chemistry modification.

Photolithographic patterning was performed using a Quintel, Inc. contact aligner. A double-layer resist system was used (lift-off resist LOR-1A overcoated by positive tone photoresist 955CM-2.1, MicroChem Corp.) which is capable of resolution at the submicrometer level. Using contact alignment, the nonpillared regions are masked off and we expose the wafer to UV light. After development, there are holes in the photoresist where the pillars will be etched. Approximately, 15−20 nm of chromium was deposited to be used as the etchant mask using an electron beam physical vapor deposition evaporator. The remaining photoresist and excess chromium is then lifted off of the wafer and all that remains on the silicon surface is the hard mask chromium areas that will not be etched. A Bosch process that alternates etching with a passivation layer of fluoropolymer was performed using anisotropic deep reactive ion etching (DRIE) to form pillars that are 15−20 μm in height (System 100 Plasma Etcher, Oxford Instruments). The Bosch process provides anisotropic etching of silicon with scalloped vertical sidewalls and, therefore, increases the surface area of our pillar sidewalls for the separation phase.[16] A thin layer of silicon oxide (~100 nm) was then deposited on the wafer surface using plasma enhanced chemical vapor deposition (PECVD) (System 100 Plasma Deposition Tool, Oxford Instruments). The pillar heights, diameters, and pitch were inspected using an FEI Dual Beam scanning electron microscope/focused ion beam (SEM/FIB) (xT Nova Nanolab 200). The processed wafers were scribed and cleaved into individual ~1 cm × 3 cm pillar array chromatographic chips prior to phase modification. A typical array is shown in Figure 2 where the images on the left are enlarged views of the array on the right to show pillar uniformity.

Surface Modification of the Silicon Oxide Surface. The deposited silicon oxide layer on the pillars served to facilitate subsequent functionalization with silane chemistry. The pillar array was first treated with equal parts of sulfuric and nitric acid to maximize the number of reactive silanol groups on the surface and was then rinsed thoroughly with distilled water and dried at 120 °C for 18 h. The stationary phase was synthesized using the method formulated by Hennion et al. which involved submerging the pillar array in pure octadecyltrichlorosilane (OTS) and heated to 170 °C for 2 h.[22] The array was then rinsed with toluene, tetrahydrofuran, a 90/10% ratio of distilled water and tetrahydrofuran, and finally distilled water. Each rinse was for 10 min and repeated twice before continuing to the next rinse stage. This method, when using Partisil packing, yields a maximum carbon content of 23%.[22] Functionalization of the pillar surface with the hydrophobic RP was verified by measuring contact angle (nonpillar area next to the array). The high contact angles observed after C18 phase modification (~135°) confirmed surface modification.

Development Chamber and Fluorescent Microscope Interface. For our initial studies, we are using fluorescence detection. To evaluate the analyte development in real time, we developed a horizontal development chamber to interface with the fluorescent microscope with a volume of approximately 2 mL. Sample development and detection can be done either simultaneously with horizontal development as performed in these experiments or can be done in the traditional vertical setup where the plate is developed and then detection is performed in a separate step. The fluorescent imaging is acquired using a Nikon Eclipse E600 and Q-capture software.

RESULTS AND DISCUSSION

Mobile Phase Velocity Comparison. Capillary action flow in TLC is governed by solvent-stationary phase adhesion and solvent surface tension. The solvent front position in a TLC development process at time t can be related to the planar chromatography system parameters using eq 2 where μ_f is the displacement of the solvent front, K_0 is the bed permeability constant, d_p is the diameter of the stationary phase particles, γ represents the surface tension, η the dynamic viscosity, and θ is the contact angle of the mobile phase.[9,23]

$$\mu_f^2 = K_0 t d_p \left(\frac{\gamma}{\eta}\right) \cos\theta \quad (2)$$

This equation has been validated by Guiochon and co-workers for a variety of TLC systems[24,25] and can be used to predict the relative velocity trend among different solvents. For the common RP solvents shown in Figure (3A) it was determined that contact angles were small and similar, thus that parameter was considered to contribute minimally to the relative velocities. Instead the solvent front velocity is mainly determined by the permeability constant and the surface tension to viscosity ratio. It has been shown that the permeability constant is much higher for pillar arrays than for more traditional systems.[9,17−20,26,27] In any case the data presented in Figure 3 is all generated with pillar diameter and pitch being equal to 2 and 4, respectively, thus K_0 is expected to be constant and the

dx.doi.org/10.1021/ac402261p | Anal. Chem. XXXX, XXX, XXX−XXX

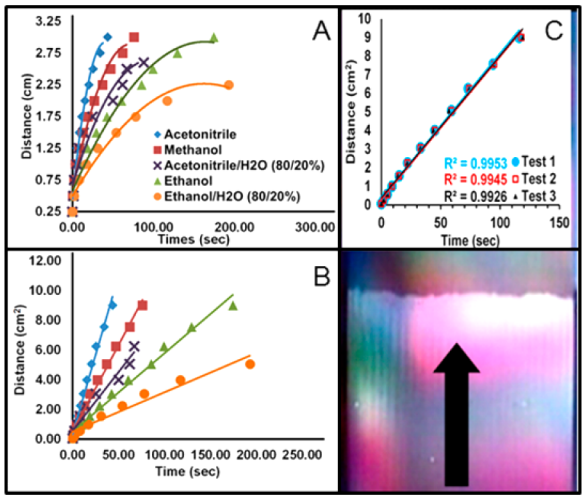

Figure 3. Solvent comparison for 2 μm diameter pillar arrays with 4 μm pitch. Part A shows the distance of the solvent as a function of time. Part B represents the squared distance data as a function of time indicating good agreement with eq 2. Part C is a typical solvent development image with an insert that shows uniformity of L^2 vs t plots.

relevant influential parameter in the solvent study is γ/η. As discussed by Poole, an increase in this ratio, as opposed to considering either value individually, is necessary to optimize the plate height for planar chromatography.[9] This ratio (see Table 2) indicates that the expected trend is consistent with

Table 2. Relevant Properties of Solvents Studied

solvent	viscosity (η) (mPa s)	surface tension (γ) (mN/m)	(γ/η)	polarity index[28] (p')
ethanol	1.07	22.4	21.5	5.2
methanol	0.54	22.5	37.9	5.1
acetonitrile	0.34	29.1	87.2	5.8

experimental results in that the acetonitrile had the greatest velocity followed by methanol, then ethanol. Also, from eq 2, the squared solvent front distance versus time is anticipated to give a linear plot and in Figure 3B we can see that the experimental results are consistent with theoretical expectations. Figure 3C illustrates that the solvent front for the planar chromatography pillar array is uniform with no apparent anomalies at the array boundaries. This is true regardless if the surrounding surface is flat unstructured Si (left) or air (right). The insert in Figure 3C indicates that the mobile phase velocity is reproducible for triplicate runs.

Flow Comparisons of Pitch Variations and to Traditional TLC. While the effect of solvent type on the flow is straightforward and predictable, the effect of pillar array morphology is a bit more intriguing and requires a more in depth look at eq 2. In TLC, the parameters γ cos θ influence the capillary action driving force for flow, which can be expected to be constant for a given TLC development process. In TLC that driving force should also scale with the packing bed surface area. Ignoring the effects of internal porosity, the surface area should increase with decreasing d_p. The value of the dynamic viscosity, η, influences the hydrodynamic flow resistance. In HPLC this flow resistance is constant and is proportional to $\nu L/d_p^2$, where ν is the mobile phase linear velocity and L is the column length. It is important to note that the flow resistance is really dependent on the sizes of the gaps between particles with smaller particles yielding smaller gaps. Thus the flow impeding quadratic effect of smaller d_p and the positive effect of smaller values on surface area, hence on the capillary driving force, can be thought to yield the overall linear d_p dependence in eq 2. In TLC, the balance of capillary action driving force and hydrodynamic resistance force is achieved early in the development process with large ν and is increasingly replaced by the longer development distance (μ_f) as the process proceeds. Our discussion here dismisses the complicating effects of hydrostatic pressure (gravity) and solvent evaporation. Engineered pillar arrays not only provide for high uniformity with a positive effect on flow (larger K_0) but also facilitate a more direct control over flow related surface area and interparticle (i.e., interpillar) gaps. With this in mind, a comparative study was performed to analyze the effect of decreasing the pitch within the system, see Figure 4A,B. The

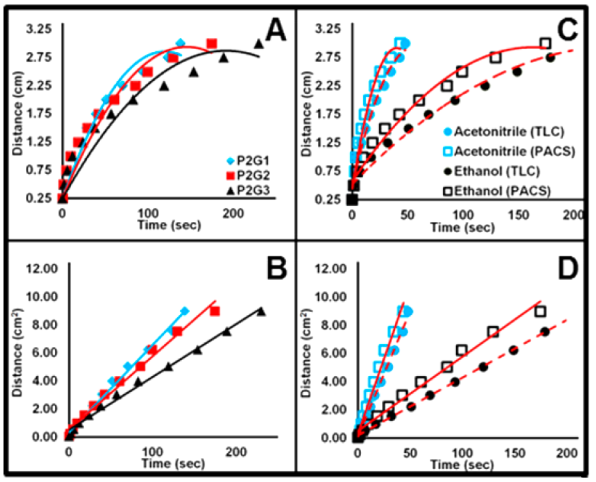

Figure 4. Parts A and B show the solvent velocity trend as the pillar diameter to pitch ratio changes, where P indicates the pillar diameter (μm) and G is the gap between pillar sidewalls (micrometers). Namely, that as the pitch to diameter ratio decreases, velocity increases. Parts C and D compare the pillar array chemical separations (PACS) to traditional TLC and indicates that although there is an order of magnitude difference in particle size, the pillar array velocity is greater than that for traditional TLC.

pillar diameter was held constant at 2 μm, and the pitch was varied to produce gaps of 1, 2, and 3 μm with ethanol used as the test solvent. The results of this study indicate that as gaps decrease for constant pillar diameter, the solvent velocity increases as seen in Figure 4A. Note that as the gap is decreased, the surface area that drives the flow process increases (see Table 2). Moreover, decreasing the gaps from 3 to 1 μm the distance that solvent must "jump" along the direction of flow between isolated pillars decreases, which may be thought to effectively increase the permeability parameter K_0. The high aspect ratio of the pillars minimize chip floor affects and the capillary flow between the pillars is probably the dominating force. It is certainly true that the hydrodynamic flow resistance increases as the gap decreases but not with a quadratic dependency as predicted by the Poiseuille relationship for flow in a simple capillary tube.[29] The net effect of these factors is a counterintuitive increase in flow with decreasing system size (specifically interpillar gaps) as shown in Figure 4.

To further highlight the advantages of the 2 μm pillar array system with 2 μm gaps (P2G2) when compared to

dx.doi.org/10.1021/ac402261p | Anal. Chem. XXXX, XXX, XXX−XXX

conventional TLC plates, the solvent velocity of a reverse phase TLC plate (Sigma Aldrich C18 silica gel matrix) was recorded using both acetonitrile and ethanol. The solvents were chosen because they represented the range of the surface tension to viscosity ratio shown in Table 2. For both solvents, the pillar array systems showed an increase in mobile phase velocity over the TLC plates. This increase while modest occurs despite almost an order of magnitude greater TLC particle size compared to the pillar dimensions. Implications of which on efficiency will be discussed later.

Analyte Spotting Methods and Reproducibility. Critical spotting parameters include sample spot size and reproducibility. Since the overall pillar array size is smaller than typical TLC plates and our goal is high efficiency, very small sample spots are of paramount importance. Several methods of introducing small spot sizes onto UTLC or TLC substrates have been reported which allow spotting in the low- to submm regime.[30−33] Manipulation of the superhydrophobic nature of our chromatographic system negated the need to use these more elaborate spotting methods. Analytes of interest for chromatographic systems are often only soluble in organic solvents. Spotting with organic solvents on the hydrophobic RP leads to a very large initial spot. To counteract this affect we dissolved our test analytes (standard fluorescent dyes) in methanol and then diluted these samples using aqueous solvents (water or high water content). Two spotting methods that exploit the super hydrophobic character of the arrays were explored; droplet release (from a 1 μL HPLC syringe)/evaporation (Figure 5A) and contact transfer (Figure 5B, upper).

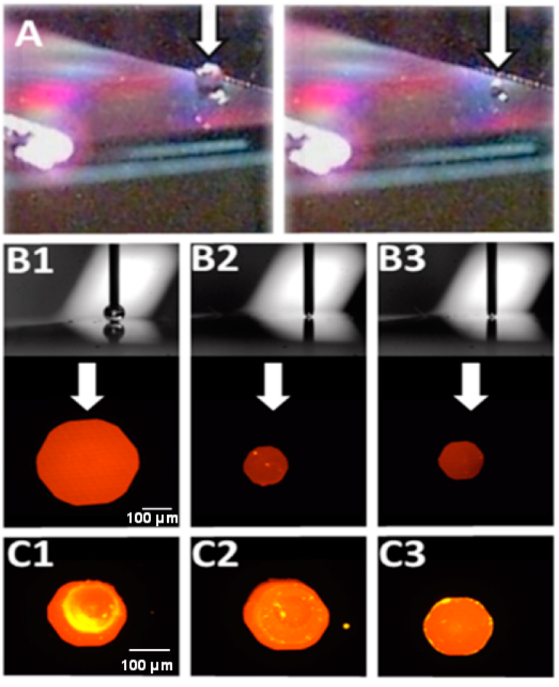

Figure 5. Droplet release spotting method is demonstrated in part A while contact spotting with spot size control is seen in parts B1−B3. Parts C1−C3 show the reproducibility of the contact spotting method.

With droplet release it was anticipated that as the droplet evaporates the super hydrophobic mode would shift from the Cassie state, riding on the pillars, to the Wenzel, falling into the pillars.[34] An issue with this technique is that it was difficult to place the droplet in a precise location on the array. Also, with the RP modified pillars, the Wenzel mode was often not cleanly observed, hence it is doubtful the sample penetrates the underlying pillars. The contact transfer spotting method was designed using the 1 μL HPLC syringe and a CCD camera to assist in visualization. Using this approach, the analyte droplet could easily be placed in specific regions of the array without damaging the pillars with the syringe tip. Fluorescent images of this spotting method indicate that controlling the droplet volume and contact time allows for sample application of varying spot sizes (Figure 5B-lower).

Initial fluorescent microscope imaging indicated that this method was successful; however, upon further investigation it was determined that the images were misleading. Although the spots appeared to be of an appropriate diameter, symmetrical and reproducible the fluorescent images were representative of the contact of the dye with the tops of the pillar. On some occasions, the spots take a polygonal shape that mimics the pillar geometry, an effect that has been described by a "pinning" effect during imbibition which causes the solvent droplet to mimic the shape of the pillars within an array at appropriate aspect ratios.[35] However, as with the droplet release method, the hydrophobic nature of the C18 phase and the microstructure pillars discouraged samples of analyte in pure water from entering the pillar array, therefore the underlying spot shape and degree of true analyte loading was uncertain. It is important to note that during the development process the moving solvent front does not wet the pillar tops, something that is easily observed by noting the spot before and after development. This issue was addressed by adding RP organic modifier to the analyte solution in controlled ratios to determine the appropriate percentage of modification while maintaining a small spot diameter. It was determined that 50−60% methanol modification allowed for the dye to enter the pillar array while maintaining sufficient hydrophilic nature to maintain small spots. This percentage could change if the array and surface modification is changed. Average spot sizes of approximately 200 μm in diameter were reproducibly observed as shown in Figure 5C.

Efficiency Analysis: Plate Height versus μ_f Position. While factors that contribute to plate height, H, are extremely complex in planar chromatography,[9,19] the treatment by Guiochon[36] is generally regarded as comprehensive and is based on the validity of the Van Deemter equation (eq 3) that is common to HPLC theory.

$$H = A + \frac{B}{v} + (C_S + C_M)v \tag{3}$$

Generally, plate height is dependent on eddy diffusion, A, longitudinal diffusion, B, which is influenced by the mobile phase velocity (v) and resistance to mass transfer in both the stationary and mobile phases, C_S and C_M, respectively. Expansion of the Van Deemter equation to include the parameters that influence plate height is shown in eq 4.

$$H = 2\lambda d_p + \frac{2\lambda D_M}{v} + \frac{qk' {d_f}^2 v}{(1+k')^2 D_S} + \frac{\omega {d_p}^2 v}{D_M} \tag{4}$$

In this equation the critical particle diameter is represented by d_p, the partition coefficient is k', the average film thickness of the stationary phase is d_f, the diffusion coefficients for the stationary and mobile phases are D_S and D_M, and independent

dx.doi.org/10.1021/ac402261p | Anal. Chem. XXXX, XXX, XXX−XXX

factors that are specific to the column packing include q, λ, γ, ω.[16,37]

The eddy diffusion term (A) can be excluded from consideration in the case of perfectly ordered pillar arrays.[15] Also, any broadening contributions from the stationary phase term (C_S) can be excluded for the simplifying case of an unretained solute ($k' = 0$). Using experimental literature values for pillar arrays, we previously reported for γ (0.5) and ω (0.02),[15] the relevant plate height can be estimated based solely on the ubiquitous B and C_M terms by using eq 5.[15,38,39]

$$H = \frac{2(0.5)D_M}{v} + \frac{0.02{d_p}^2 v}{D_M} \quad (5)$$

Employing a typical diffusion coefficient (D_M) of 5.0×10^{-6} cm^2/s for the solute and experimental velocities for both the pillar array and the traditional TLC plate (see Figure 4) we can compare the predicted plate heights for each system based on position of the solvent front μ_f (Figure 6A).

For the pillar array system, plate heights are predicted to be significantly smaller than the TLC plates when using identical parameters for the packing factors and only changing the critical particle size (d_p) value and using the experimental velocities. In this case, the TLC d_p is taken as the manufacturer's value of 10 μm and polydispersity is not considered. For the pillar array system, d_p is taken as the more relevant 1 μm gap. In both systems, the solute band is assumed to be located at the advancing solvent front but not spatially altered by its proximity to the front. In these treatments of relative efficiency, the difference between the plate heights of these two systems would be expected to be much greater than shown if the actual packing factor terms for TLC were to be used and, in particular, when the eddy diffusion term is also included. Since the linear flow velocity for the pillar array chemical separations (PACS) system is only slightly greater than the TLC case, Figure 4C,D, at large distances the efficiencies shown in Figure 6A are dominated by diffusion. Under these conditions, the array platform is only roughly a factor or two better than the TLC case. It is at small distances (rapid flow) that a dominance of the C_M term occurs and the TLC efficiency suffers greatly as seen from the upturn of H shown in the figure. If one were to use smaller particles for TLC to counteract the C_M problem, reductions in flow as predicted by eq 2 would exacerbate diffusion problems. Conversely, the unique flow characteristics of the pillar arrays permit small diameter pillars and interpillar gaps without evidence of C_M issues for pillar array systems. This behavior is seen when comparing the three different gap sizes shown in Figure 6B. For all three gaps there is no significant evidence of C_M issues and at longer solvent front distance the fastest moving 2 μm pillar diameter arrays with 1 μm gaps (P2G1) is most efficient. In this treatment we have not considered possible nondevelopment sources of band dispersion; e.g., sample application and detection processes and possible slow solvation as the solvent front encounters sample spots.

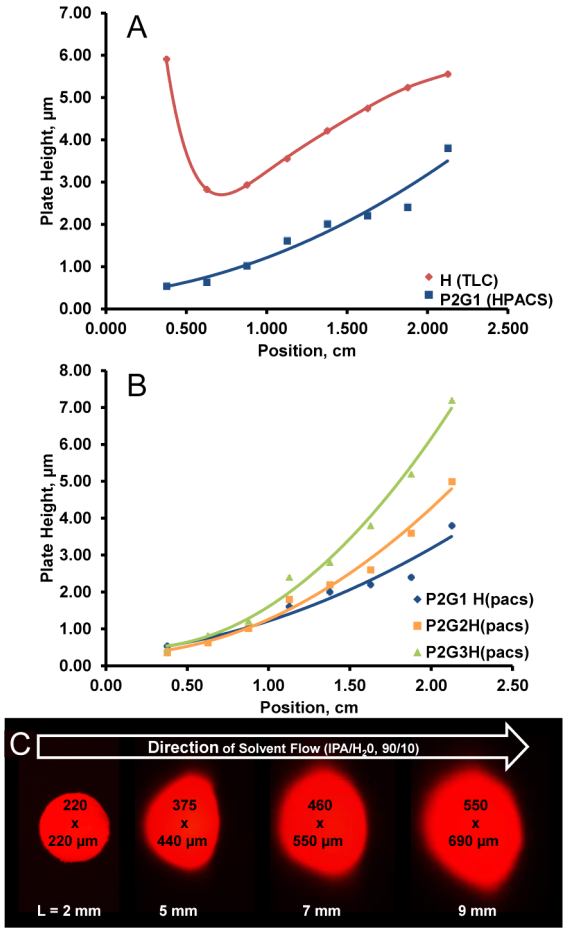

Figure 6. Van Deemter-like plots of flow rate linear flow velocity dependent on the solvent front versus B and C_M term-based plate height. Experimental flow rates linear flow velocities are taken from the exponential fits in Figure 4A,C. The predicted superior performance of a PACS versus a commercial TLC plate is shown in parts A and B and demonstrates the effect of PACS gap size, where P represents the pillar diameter (μm) and G indicates the gap betweeen the pillar sidewalls (micrometers). (C) Evaluation of R6G in real time giving H values of 1.0, 1.4, and 1.7 μm, respectively, from the original spot at 2 mm.

Preliminary Experimental Evaluation of Plate Height. An example of band dispersion captured in real time as the analyte moves through the P2G1 pillar array is shown in Figure 6C. The analyte is rhodamine 6G (1×10^{-7} M) applied from a 50/50% methanol/H_2O solution to create a 220 μm diameter spot located 2 mm from the edge of the array. The mobile phase used for development is isopropanol/water (90/10%). A fluorescence microscope signal acquisition time of 1 s allowed for the observation of the analyte at low concentrations without observing a noticeable blurring effect. Spot dispersion in the direction of solvent flow is minimized in this experiment due to the concentrating effect of the analyte being very near the solvent front, so efficiency was evaluated in the direction perpendicular to that flow. Using these measured spot sizes we expect that diffusion (B-term) is being evaluated and that is deemed appropriate by the treatment in Figure 6A,B. Although the bands (especially original spot) are not Gaussian in shape and the actual spot sizes are prone to interpretation, we use $H = \sigma^2$/distance developed to estimate efficiency with σ equal to one-fourth of the apparent spot size; for example, $H_{2-5} = (115-55)^2/3000 = 1.2$ μm. Similarly for the spots seen at 7 and 9 mm we have $H_{2-7} = 1.7$ μm, and $H_{2-9} = 2.0$ μm, respectively, as estimates of plate height ($k \approx 0$).

Comparing these values with the expected plate heights in Figure 6B, the trend of increasing H with slower flow is seen but the actual observed plate heights are a little higher than what was predicted. This could reflect our crude method of evaluating H. More likely, this can be explained by considering the band broadening introduced by nondevelopment factors,

dx.doi.org/10.1021/ac402261p | Anal. Chem. XXXX, XXX, XXX−XXX

in this case solvation of the analyte spot during the initial confrontation with the moving solvent front. Considering band dispersion from both spot solvation (SS) and development factors (DF) as discussed in the previous section, plate height can be reduced to eq 6.

$$H = H_{SS} + H_{DF} \quad (6)$$

The uniformity of the pillar array and the low concentration of rhodamine 6G should minimize H_{SS} as compared to TLC. Still it is unreasonable to expect it to be negligible, particularly with the rapid flow early in the development process. As is so often the case, chromatography is a compromise; in this manifestation, spot close to the edge of the array to minimize H_{DF} (B-term here) but spot far from the edge to minimize H_{SS}. Regardless of the rather crude methods of evaluating efficiency used herein, it is clear the initial and developed spots are very small compared to TLC and follow expected trends.

CONCLUSION

The research presented herein, for the first time demonstrates that lithographically produced highly ordered pillar arrays can be used as reusable planar chromatography separation platforms that employ simple capillary flow as the driving force. Both practical and fundamental aspects are discussed and illustrated herein. This open system bypasses issues observed in pressurized pillar array chromatography including sealing of the system. We have incorporated an effective C18 stationary phase functionalization of the arrays that does not cause occlusion between the pillars. Linear flow velocity studies during development reveal a somewhat surprising trend to more rapid flow as pillar size and gap decrease. Rationalization of this trend and its effect on efficiency is presented and point to the value of pillar arrays when compared to more traditional planar platforms for separations. By taking advantage of the superhydrophobic nature of the system we are able to apply sample in very small spots and image the spots and separations with a simple fluorescence microscope. The promising results of these initial studies motivate further reduction in system size, exploration of stationary phases, and modeling in our future work.

AUTHOR INFORMATION

Corresponding Author

*E-mail: msepaniak@utk.edu.

Author Contributions

Michael Sepaniak is the principal investigator, project director, and corresponding author; Nickolay Lavrik and Nahla A. Hatab contributed to fabrication; and Teresa Kirchner contributed to all aspects.

Notes

The authors declare no competing financial interest.

ACKNOWLEDGMENTS

This material is based upon work supported by the National Science Foundation under Grant No. 1144947. A portion of this research was conducted at the Center for Nanophase Materials Sciences, which is sponsored at Oak Ridge National Laboratory by the Scientific User Facilities Division, Office of Basic Energy Sciences, U.S. Department of Energy.

REFERENCES

(1) Gzil, P.; Vervoort, N.; Baron, G. V.; Desmet, G. *Anal. Chem.* **2003**, *75*, 6244−6250.
(2) De Malsche, W.; Clicq, D.; Verdoold, V.; Gzil, P.; Desmet, G.; Gardeniers, H. *Lab Chip* **2007**, *7*, 1705−1711.
(3) De Malsche, W.; Eghbali, H.; Clicq, D.; Vangelooven, J.; Gardeniers, H.; Desmet, G. *Anal. Chem.* **2007**, *79*, 5915−5926.
(4) De Smet, J.; Gzil, P.; Vervoort, N.; Verelst, H.; Baron, G. V.; Desmet, G. *Anal. Chem.* **2004**, *76*, 3716−3726.
(5) He, B.; Regnier, F. *J. Pharm. Biomed. Anal.* **1998**, *17*, 925−932.
(6) Regnier, F. E. *J. High Resolut. Chromatogr.* **2000**, *23* (1), 19−26.
(7) Eghbali H.; De Malsche W.; Clicq D.; Gardeniers H.; Desmet G. *LC−GC Eur.* **2007**, *20*.
(8) Schure, M. R.; Maier, R. S.; Kroll, D. M.; Davis, H. T. *J. Chromatogr., A* **2004**, *1034*, 79−86.
(9) Poole, S. K.; Poole, C. F. *J. Chromatogr., A* **2011**, *1218*, 2648−2660.
(10) Huang, L. R.; Cox, E. C.; Austin, R. H.; Sturm, J. C. *Science* **2004**, *304* (5673), 987−990.
(11) De Malsche, W.; Gardeniers, H.; Desmet, G. *Anal. Chem.* **2008**, *80*, 5391−5400.
(12) Eghbali, H.; Matthijs, S.; Verdoold, V.; Gardeniers, H.; Cornelis, P.; Desmet, G. *J. Chromatogr., A* **2009**, *1216*, 8603−8611.
(13) Tiggelaar, R. M.; Verdoold, V.; Eghbali, H.; Desmet, G.; Gardeniers, J. G. E. *Lab Chip* **2008**, *9*, 456−463.
(14) De Malsche, W.; De Bruyne, S.; De Beeck, J. O.; Eeltink, S.; Detobel, F.; Gardeniers, H.; et al. *J. Sep. Sci.* **2012**, *35*, 2010−2017.
(15) Lavrik, N. V.; Taylor, L. C.; Sepaniak, M. J. *Lab Chip* **2010**, *10*, 1086−1094.
(16) Taylor, L. C.; Lavrik, N. V.; Sepaniak, M. J. *Anal. Chem.* **2010**, *82*, 9549−9556.
(17) Clark, J. E.; Olesik, S. V. *Anal. Chem.* **2009**, *81*, 4121−4129.
(18) Bezuidenhout, L. W.; Brett, M. J. *J. Chromatogr., A* **2008**, *1183*, 179−185.
(19) Poole, C. F. *J. Chromatogr., A* **2003**, *1000*, 963−984.
(20) Sherma, J. *Anal. Chem.* **2004**, *76* (12), 3251−3470.
(21) Daneyko, A.; Hlushkou, D.; Khirevich, S.; Tallarek, U. *J. Chromatogr., A* **2012**, *1257*, 98−115.
(22) Hennion, M. C.; Picard, C.; Caude, M. *J. Chromatogr.* **1978**, *166*, 21−35.
(23) Saha, A. A.; Mitra, S. K.; Tweedie, M.; Roy, S.; McLaughlin, J. *Microfluid. Nanofluid.* **2009**, *7*, 451−465.
(24) Guiochon, G. *J. Chromatogr., A* **2007**, *1168*, 101−168.
(25) Guiochon, G.; Korosi, G.; Siouffi, A. *J. Chromatogr. Sci.* **1980**, *18*, 324−329.
(26) Kauppila, T. J.; Talaty, N.; Salo, P. K.; Kotiaho, T.; Kostiainen, R.; Cooks, G. *Rapid Commun. Mass Spectrom.* **2006**, *20*, 2143−2150.
(27) Tuomikoski, S.; Huikko, K.; Grigoras, K.; Ostman, P.; Kostiainen, R.; Baumann, M.; et al. *Lab on a Chip.* **2002**, *2*, 247−253.
(28) Snyder, L. R. In *Techniques of Chemistry, III*; Weissberger, A., Perry, E. S., Eds.; Wiley-Interscience: New York, 1978.
(29) Washburn, E. W. *Phys. Rev.* **1921**, *17* (3), 273−283.
(30) Streule, W.; Lindemann, T.; Birkle, G.; Zengerle, R.; Koltay, P. *J. Assoc. Lab. Automation* **2004**, *9*, 300−306.
(31) Powell, S. C. *Anal. Chem.* **2010**, *82*, 3408−3408.
(32) Fenimore, D. C.; Meyer, C. J. *J. Chromatogr.* **1979**, *186*, 555−561.
(33) Byun, C. K.; Wang, X.; Pu, Q.; Liu, S. *Anal. Chem.* **2007**, *79*, 3862−3866.
(34) Koishi, T.; Yasuoka, K.; Fujikawa, S.; Ebisuzaki, T.; Zeng, X. C. *Proc. Natl. Acad. Sci. U.S.A.* **2009**, *106* (21), 8435−8440.
(35) Courbin, L.; Denieul, E.; Dressaire, E.; Roper, M.; Ajdari, A.; Stone, H. A. *Nat. Mater.* **2007**, *6*, 661−664.
(36) Guiochon, G.; Antoine, S. *J. Chromatogr. Sci.* **1978**, *16*, 470−481.
(37) Lavrik, N. V.; Taylor, L. T.; Sepaniak, M. J. *Anal. Chim. Acta* **2011**, *694*, 6−20.
(38) Deininger, G. *Chromatographia* **1976**, *9* (6), 251−254.
(39) Poole, C. *The Essence of Chromatography*; Elsevier Science B.V.: Amsterdam, The Netherlands, 2003.